METALS AND MATERIALS International, Vol. 11, No. 5 (2005), pp. 351~355

Processing and Mechanical Properties of Porous Silica-Bonded Silicon Carbide Ceramics

Yong-Seong Chun and Young-Wook Kim*

Department of Materials Science and Engineering, the University of Seoul, 90 Jeonnong-dong, Dongdaemun-gu, Seoul 130-743, Korea

A simple processing route for manufacturing highly porous, silica-bonded SiC ceramics with spherical pores has been developed. The strategy adopted for making porous silica-bonded SiC ceramics entails the following steps: (i) fabricating a formed body through a combination of SiC and polymer microbeads (employed as sacrificial templates) and (ii) sintering the formed body in air. SiC particles are bonded to each other by oxidation-derived SiO_2 glass. By controlling the microbead content and the sintering temperature, it was possible to adjust the porosity such that it ranged from 19 to 77 %. The flexural and compressive strengths of the porous silica-bonded SiC ceramics with ~40 % porosity were ~65 MPa and ~200 MPa, respectively. The superior strengths were attributed to the homogeneous distribution of small ($\leq$ 30 μm), spherical pores with dense struts in the porous silica-bonded SiC ceramics.

Keywords: Porous materials, Silicon carbide, Processing, Strength

1. INTRODUCTION

Porous SiC ceramics are used widely as a structural and refractory ceramic material because of their intrinsic high strength, good chemical stability, excellent thermal shock resistance, and good creep resistance at high temperatures [1-3]. Among the various applications of porous SiC ceramics, catalyst supports, hot-gas filters, and molten-metal filters have received considerable attention in recent years [4-6].

Porous SiC ceramics can be fabricated by a variety of methods including replication [7] and space holder approaches [8,9], partial sintering [10], and use of the carbothermal reduction route of polysiloxanes [11]. However, the heat-treatment step of these methods is conducted in an inert atmosphere. Recently, She et al [2,12,13] developed an oxidation-bonding technique for the fabrication of porous SiC ceramics. In this process, the powder compacts are heated in air instead of an inert atmosphere. Because of the occurrence of surface oxidation during heat-treatment, SiC particles bond to each other by the oxidation-derived SiO_2 glass. High strength, i.e., up to ~185 MPa, was achieved at a porosity of 31 % [12]. By adding graphite as a sacrificial template, they could control porosity in a range of 30 to 70 % [2].

Since pore morphology and porosity (i.e., pore size and pore size distribution) directly impact a material's ability to perform desired functions in a particular application, it is desirable to fabricate a porous ceramic structure of regulated pore-size and porosity [14-16]. This paper describes a simple process for preparing highly porous, silica-bonded SiC ceramics with spherical pores. The spherical pore structure was achieved by means of a sacrificial templating agent (polymer microbeads). A spherical pore structure would be beneficial with respect to the mechanical properties of porous ceramics because it would reduce stress concentration at sharp crack tips. Heat-treatment of SiC powder compacts in air leads to the formation of amorphous SiO_2 on the surface of SiC particles, which enables the formation of bonding between SiC particles at relatively low temperatures. By controlling the heat-treatment temperature and the microbead content, it was possible to adjust the porosity of porous silica-bonded SiC ceramics such that it ranged from 19 to 77 %. The porosity dependence of the compressive and flexural strengths of the resulting porous ceramics was also investigated.

2. EXPERIMENTAL PROCEDURE

A commercially available β-SiC powder (~0.34 μm, Ultrafine grade, Betarundum, Ibiden Co. Ltd, Ogaki, Japan) and poly (methyl methacrylate-co-ethylene glycol dimethacrylate) microbeads (~20 μm, Sigma-Aldrich Inc, St. Louis, MO) (designated as polymer microbeads) were used as raw materials. Eight batches of powders were mixed and the content of microbeads in the batches ranged from 0 to 80 vol.%

*Corresponding author: ywkim@uos.ac.kr

Table 1. Batch composition and sample designation

Sample	Batch composition			
	wt.%		vol.%	
	SiC*	Microbead**	SiC	Microbead
SSC0	100	0	100	0
SSC2	91.5	8.5	80	20
SSC3	86.3	13.7	70	30
SSC4	80.2	19.8	60	40
SSC5	73.0	27.0	50	50
SSC6	64.3	35.7	40	60
SSC7	53.7	46.3	30	70
SSC8	40.3	59.7	20	80

*~0.34 μm, Untrafine, Ibiden Co., Lyd, Nagoya, Japan.
**poly(methyl methacrylate-co-ethylene glycol dimethacrylate) microbeads, ~20 μm, Sigma-Aldrich Inc, St. Louis, MO.

(Table 1). All individual batches were mixed in ethanol for 12 h using Teflon balls and a polyethylene jar after 2 wt.% poly (ethylene glycol) addition as a binder. The mixed slurry was dried and uniaxially pressed into rectangular hexahedrons with dimensions of 25 × 30 × 8 mm at 20 MPa. The green compacts were heat-treated at temperatures ranging from 1300 to1400 ℃ for 1 h at a heating rate of 2 ℃/min in air.

The bulk density (D_b) of the porous SiC ceramics was computed from the weight-to-volume ratio. The theoretical density (D_{th}) of silica-bonded SiC was estimated by the rule of mixtures:

$$D_{th} = (1 - V_{SiO_2}) D_{SiC} + V_{SiO_2} D_{SiO_2} \quad (1)$$

where D_{SiC} and D_{SiO_2} are the theoretical densities of SiC (3.2 g/cm^3) and SiO_2 (2.3 g/cm^3), and V_{SiO_2} is the volume fraction of SiO_2 in the specimen. V_{SiO_2} was calculated from the weight change of the specimen during heat-treatment in air [12]. The porosity of the porous ceramics was calculated from the bulk density of the porous ceramics and the theoretical density (D_{th}) of the strut material according to:

$$\text{Porosity (\%)} = (1 - D_b/D_{th}) \times 100 \quad (2)$$

The pore morphology was observed by scanning electron microscopy (SEM). Using CuKα radiation, X-ray diffractometry (XRD) was performed on ground powders. The compressive strength was measured using a cross-head speed of 0.5 mm/min on samples with a size of 3 × 3 × 6 mm. A total of 116 specimens with porosities ranging from 19 to 77 % were measured. For the flexural strength measurements, bar-shaped samples were machined to a size of 3 × 4 × 30 mm. Bend tests were performed at room temperature using a four-point method with an inner and outer span of 10 and 20 mm, respectively. A total of 70 specimens with porosities ranging from 19 to 70 % were measured using a crosshead speed of 0.5 mm/min.

3. RESULTS AND DISCUSSION

SiC powder compacts containing polymer microbeads were heated to a temperature ranging from 1300 to 1400 ℃ followed by isothermal holding at the same temperature. This process allows (1) burn-out of the polymer microbeads, leaving spherical pores in the compacts; and (2) oxidation of SiC powders, forming oxidation-derived silica as a bonding phase between SiC particles, resulting in porous silica-bonded SiC ceramics. Phase analysis by XRD showed the presence of only β-SiC as a crystalline phase, indicating the formation of amorphous SiO_2 as an oxidation product of SiC. Densification of the strut may start between 800-1000℃, and likely

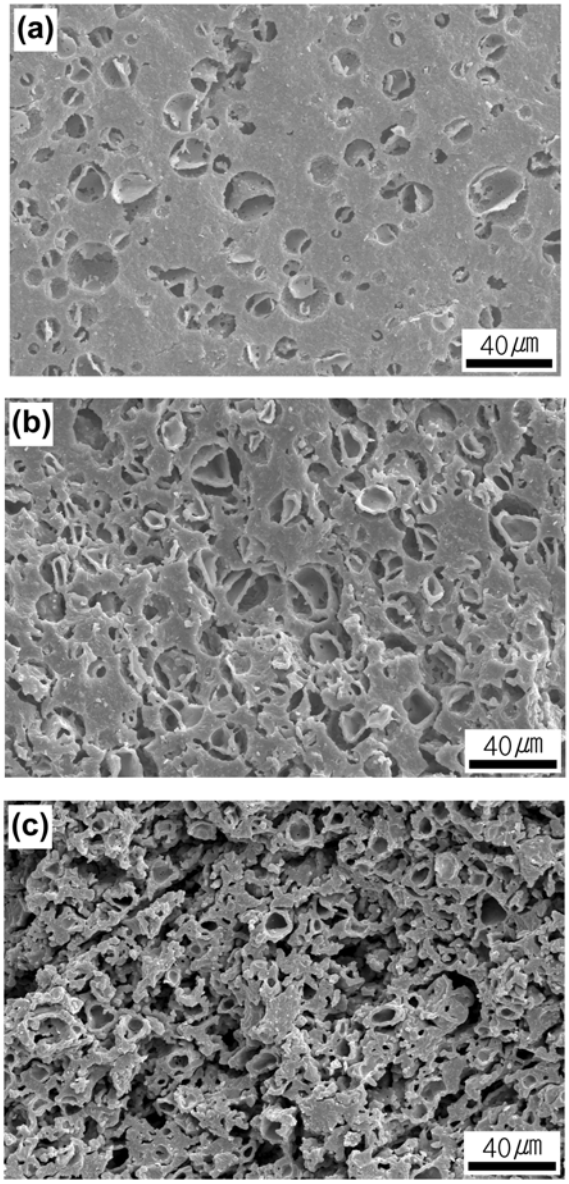

Fig. 1. Typical fracture surfaces of porous silica-bonded SiC ceramics sintered at 1400 ℃ for 1 h in air: (a) SSC3, (b) SSC6, and (c) SSC8 (refer to Table 1).

follows a similar mechanism as that proposed for the sintering of amorphous SiO_2 by a viscous sintering process [17].

Typical fracture surfaces of porous silica-bonded SiC ceramics are shown in Fig. 1. As shown, fine, well-distributed pores and dense struts were achieved. When the microbead loading was ≥ 60 vol.%, interconnected open pores were formed whereas isolated spherical pores were formed when the microbead loading was ≤ 50 vol.%. The pore morphology changed from closed to open as the microbead content increased in the porous ceramics; this change was due to the greater opportunity for contact between microbeads in the compacts with ≥ 60 vol.% microbead loading (compare Fig. 1(a) with Fig. 1(c)). The morphology of pores replicated from the polymer microbeads was almost spherical, indicating that the shape of the polymer microbeads was retained in the SiC-polymer microbead compacts up to their decomposition temperature. However, some of the interconnected pores were not spherical in the porous silica-bonded SiC ceramics with 80 vol.% microbead loading (Fig. 1(c)). The maximum pore size was below 30 μm, and there were no large voids in the bulk materials. This suggests that the proposed processing method does not suffer from significant agglomeration of the polymer microbeads and, at the same time, allows for uniform distribution of SiC particles among the sacrificial templates.

Fig. 2 shows the porosity of porous silica-bonded SiC ceramics as a function of the microbead content and the sintering temperature. The porosities recorded for the silica-bonded SiC ceramics yielded in this experiment ranged from 25 to 77 % for the 1300 °C-sintered specimens, from 21 to 69 % for the 1350 °C-sintered specimens, and from 19 to 58 % for the 1400 °C-sintered specimens. It should be noted that these ranges depended on both the microbead content and the sintering temperature. Porosity varied directly with the microbead content for all observed specimens (i.e., higher microbead content corresponded with higher porosity). It is expected that higher microbead content leads to a larger number of pores, resulting in higher porosity. In contrast, higher sintering temperature led to lower porosity due to enhanced densification at the higher temperature. Thus, by controlling the microbead content and the sintering temperature, it was possible to control the porosity of the porous silica-bonded SiC ceramics within a range of 19 to 77 %. The optimum range of porosity for the applications noted in the

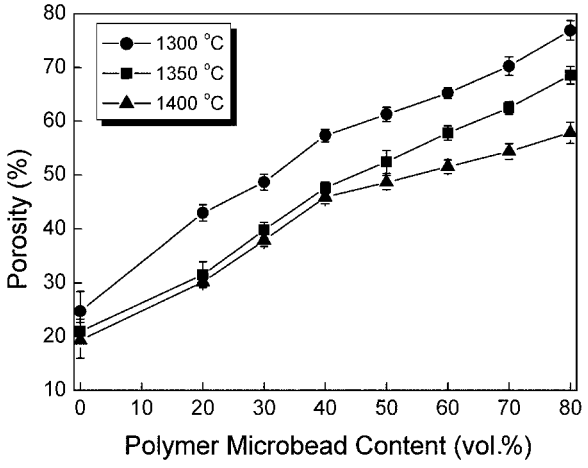

Fig. 2. Porosity of porous silica-bonded SiC ceramics as a function of microbead content.

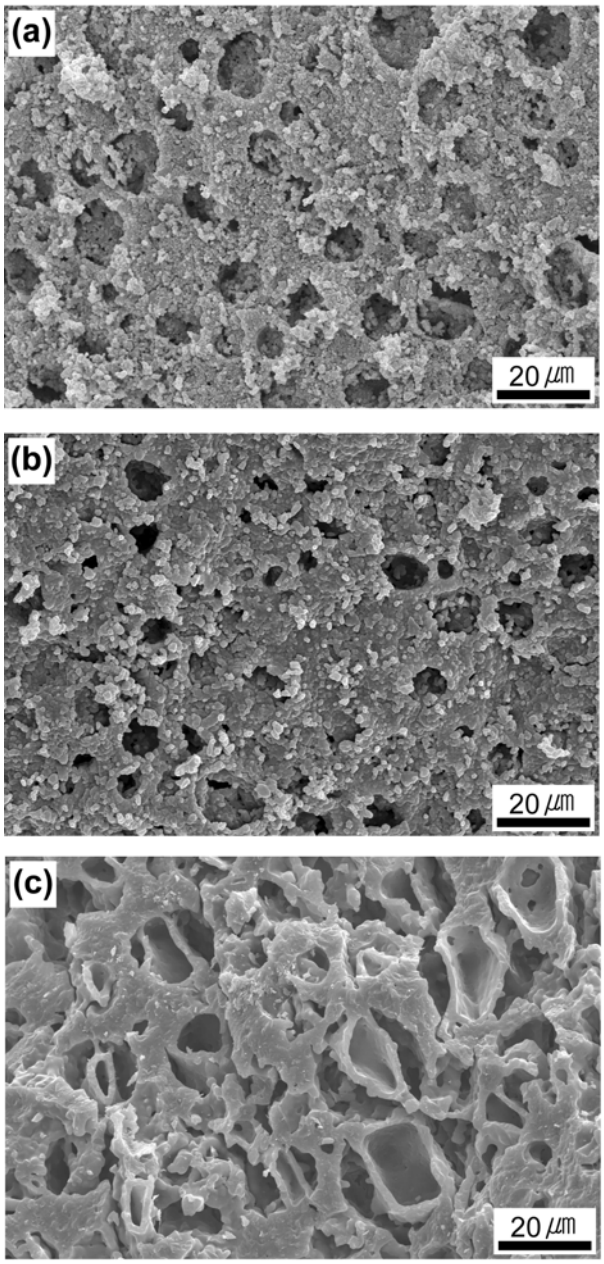

Fig. 3. Typical fracture surfaces of porous silica-bonded SiC ceramics (SSC6) sintered at various temperatures for 1 h in air: (a) 1300 °C, (b) 1350 °C, and (c) 1400 °C.

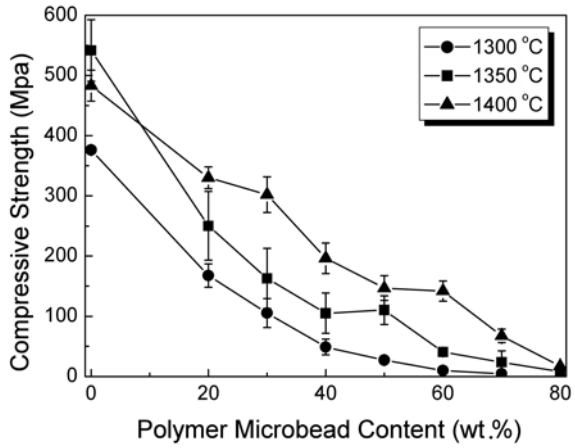

Fig. 4. Compressive strength of porous silica-bonded SiC ceramics as a function of microbead content.

introductory section is considered to be 40~75 %, depending on their design and size. Thus, the porosity obtained in the present study covers the range fully.

Some typical microstructures of porous silica-bonded SiC ceramics (SSC6) sintered at 1300, 1350, and 1400 °C for 1 h in air are shown in Fig. 3. The porosity decreased from 65 % for the 1300 °C-sintered specimen to 52 % for the 1400 °C-sintered specimen. Higher sintering temperature was associated with higher bulk density. Since the oxidation kinetics are faster at higher temperatures, a larger amount of oxidation-derived SiO_2 is formed at 1400 °C. In addition, the oxidation-derived SiO_2 accelerates particle rearrangement and densification by a viscous sintering process, leading to dense struts and less porosity. The maximum pore sizes in all specimens ranged from 25 to 30 μm, suggesting that the pores were formed from the added polymer microbeads.

Fig. 4 illustrates the compressive strength as a function of polymer microbead content for the samples sintered at 1300-1400 °C. As shown, the strength decreased as the microbead content increased. This tendency is opposite to that of the porosity change with the microbead content (Fig. 2), indicating that porosity controls the strength of the silica-bonded SiC ceramics. Generally, the specimens sintered at higher temperatures exhibited higher compressive strength at the same microbead loading. The superior strength achieved at higher sintered temperature is attributed to the beneficial effect of oxidation-derived SiO_2 with respect to the densification of the strut and enhanced densification at higher temperature at the same microbead loading.

Fig. 5 presents the compressive and flexural strength data as a function of the volume fraction of pores. Both the compressive and the flexural strength decreased with increased porosity. According to a model proposed by Rice [18], the strength of a porous material is related to its porosity through the expression

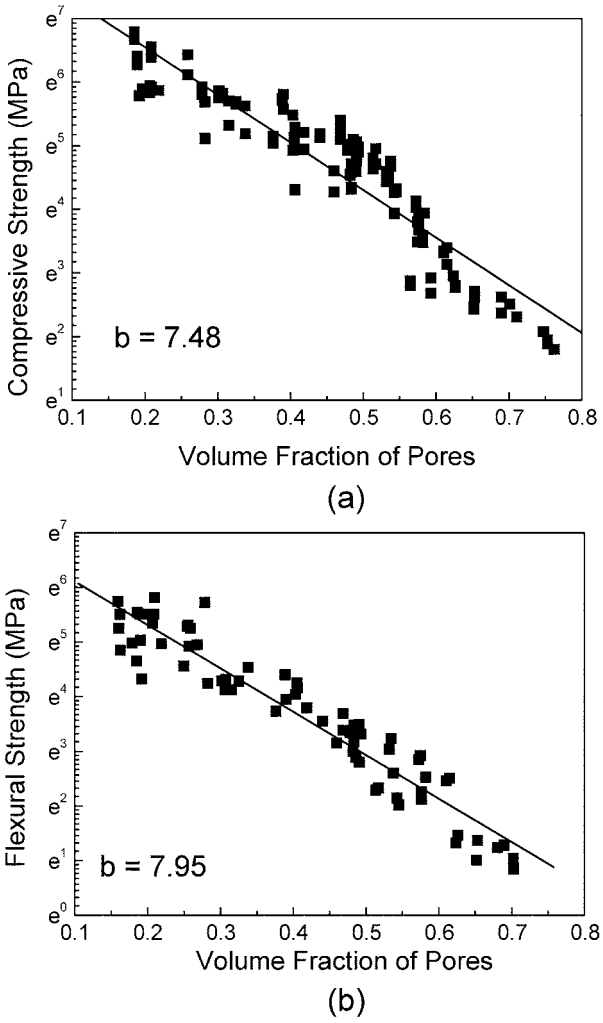

Fig. 5. Compressive and flexural strength data of porous silica-bonded SiC ceramics as a function of pore volume fraction. Lines are a linear fit to Eq. 3.

$$\sigma = \sigma_o \exp(-b P) \quad (3)$$

where σ_o and σ are the strength of a nonporous material and the strength of a porous material with a porosity P, respectively, and b is a constant that is dependent on the pore characteristics. The values of b were reported to be 6 for cubic stacking and 9 for rhombic stacking [19]. Linear-regression fits for a plot of compressive strength versus pore volume fraction and for a plot of flexural strength versus pore volume fraction yield b = 7.48 and 7.95, respectively, for porous silica-bonded SiC ceramics. Using the rule of mixtures, the relative fraction of cubic arrangement in our specimens was estimated to be 35~51 %.

The flexural and compressive strengths of porous silica-bonded SiC ceramics with ~40 % porosities were ~65 MPa and ~200 MPa, respectively. She et al. reported a flexural strength of 185 MPa at a porosity of 31 % in a porous SiC

ceramic fabricated by an oxidation-bonding technique [12] and a flexural strength of ~40 MPa at a porosity of 36.4 % in a porous SiC ceramic doped with Al_2O_3 for enhanced neck growth via an oxidation-bonding technique [2]. It is difficult to directly compare the present data with She's data because of the differences in the measurement method and the specimen size. However, the results obtained here could be considered to be comparable or slightly superior to those of She, because four-point bending generally results in a 10-30 % lower strength value compared to three-point bending. Kim *et al.* [10] fabricated porous SiC ceramics from a SiC powder with $Y_3Al_5O_{12}$ as a sintering additive via a partial sintering process. The pore morphology was irregular in porous ceramics. The 4-point flexural strength of porous SiC ceramics with a porosity of 39 % was ~30 MPa. The superior strength of the silica-bonded SiC ceramics (~65 MPa at 40 % porosity) was attributed to the homogeneous distribution of small (> 30 μm), spherical pores with dense struts.

4. SUMMARY

Porous silica-bonded SiC ceramics with porosities ranging from 19 to 77 % were obtained from a SiC powder using polymer microbeads as a sacrificial template. The strategy adopted for making porous silica-bonded SiC ceramics with spherical pores entailed the sintering of SiC powder compacts containing microbeads as a sacrificial template in air. The sintering process in air allows: (1) burn-out of polymer microbeads, leaving spherical pores in the compacts; and (2) oxidation of SiC powders, forming oxidation-derived silica as a bonding phase between SiC particles, resulting in porous silica-bonded SiC ceramics with spherical pores.

The flexural and compressive strengths of the porous silica-bonded SiC ceramics with ~40 % porosities were ~65 MPa and ~200 MPa, respectively. The superior strengths were attributed to the homogeneous distribution of small (≤ 30 μm), spherical pores with dense struts in the porous silica-bonded SiC ceramics.

ACKNOWLEDGMENTS

This work was supported by a grant from the Center for Advanced Materials Processing (CAMP) of the 21st Century Frontier R&D Program funded by the Ministry of Commerce, Industry and Energy (MOCIE), Republic of Korea.

REFERENCES

1. S. Ito, T. Tanaka, and S. Kawamura, *Powder Tech.* **100**, 32 (1998).
2. J. H. She, Z. Y. Deng, J. Daniel-Doni, and T. Ohji, *J. Mater. Sci.* **37**, 3615 (2002).
3. Y.-W. Kim, S. H. Lee, T. Nishimura, M. Mitomo, J. H. Lee, and D.-Y. Kim, *Key Eng. Mater.* **287**, 299 (2005).
4. M. Benaissa, J. Werckmann, G. Ehret, E. Peschiera, J. Guille, and M. J. Ledoux, *J. Mater. Sci.* **29**, 4700 (1994).
5. P. H. Pastila, V. Helanti, A. P. Nikkila, and T. A. Mantyla, *Ceram. Eng. Sci. Proc.* **19**, 3744 (1998).
6. M. Keller, C. Pham-Huu, S. Roy, M. J. Ledoux, C. Estournes, and J. Guille, *J. Mater. Sci.* **34**, 3189 (1999).
7. I. K. Sung, S. B. Yoon, J. S. Yu, and D. P. Kim, *Chem. Comm.* **38**, 1480 (2002).
8. T. J. Fitzgerald and A. Mortensen, *J. Mater. Sci.* **30**, 1025 (1995).
9. T. J. Fitzgerald, V. J. Michaud, and A. Mortensen, *J. Mater. Sci.* **30**, 1037 (1995).
10. S. H. Kim, Y.-W. Kim, J.-Y. Yun, and H. D. Kim, *J. Kor. Ceram. Soc.* **41**, 541 (2004).
11. Y.-W. Kim, S. H. Kim, I. H. Song, H. D. Kim, and C. B. Park, *J. Am. Ceram. Soc.* **88**, 2949 (2005).
12. J. H. She, J. F. Yang, N. Kondo, T. Ohji, and S. Kanzaki, *J. Am. Ceram. Soc.* **85**, 2852 (2002).
13. J. H. She, T. Ohji, and S. Kanzaki, *J. Europ. Ceram. Soc.* **24**, 331 (2003).
14. Y.-W. Kim and C. B. Park, *Comp. Sci. Tech.* **63**, 2371 (2003).
15. Y.-W. Kim, S. H. Kim, C. Wang, and C. B. Park, *J. Am. Ceram. Soc.* **86**, 2231 (2003).
16. Y.-W. Kim, S. H. Kim, H. D. Kim, and C. B. Park, *J. Mater. Sci.* **39**, 5647 (2004).
17. V. Yaroshenko and D. S. Wilkinson, *J. Am. Ceram. Soc.* **84**, 850 (2001).
18. R. W. Rice, *J. Mater. Sci.* **28**, 2187 (1993).
19. F. P. Knudsen, *J. Am. Ceram. Soc.* **42**, 376 (1959).